

Supporting Information

Phage-Based Structural Color Sensors and Their Pattern Recognition Sensing System

Ju Hun Lee,^{1,2} Benson Fan,³ Tuan D. Samdin,⁴ David A. Monteiro,^{1,5} Malav S. Desai,^{1,2} Olivia Scheideler,^{1,2} Hyo-Eon Jin,^{1,2,8} Soyoun Kim,⁶ Seung-Wuk Lee^{*,1,2,7}.

AUTHOR ADDRESS.

¹Department of Bioengineering, University of California, Berkeley, CA 94720, United States

²Biological Systems and Engineering, Lawrence Berkeley National Laboratory, Berkeley, CA 94720, United States

³Bioinspira Inc., Berkeley, CA 94720

⁴Department of Molecular and Cell Biology, University of California, Berkeley, CA 94720, United States

⁵University of California, Berkeley–University of California, San Francisco Graduate Program in Bioengineering, University of California, Berkeley, CA 94720, United States

⁶Department of Biomedical Engineering, Dongguk University, Seoul 04620, Republic of Korea

⁷Tsinghua-Berkeley Shenzhen Institute, Shenzhen, People's Republic of China.

⁸College of Pharmacy, Ajou University, Suwon 16399, Republic of Korea.

KEYWORDS. M13 bacteriophage, Columnar smectic phase, Cross-reactive, Structural Color,

Biomimetics, Biosensor, Olfactory system

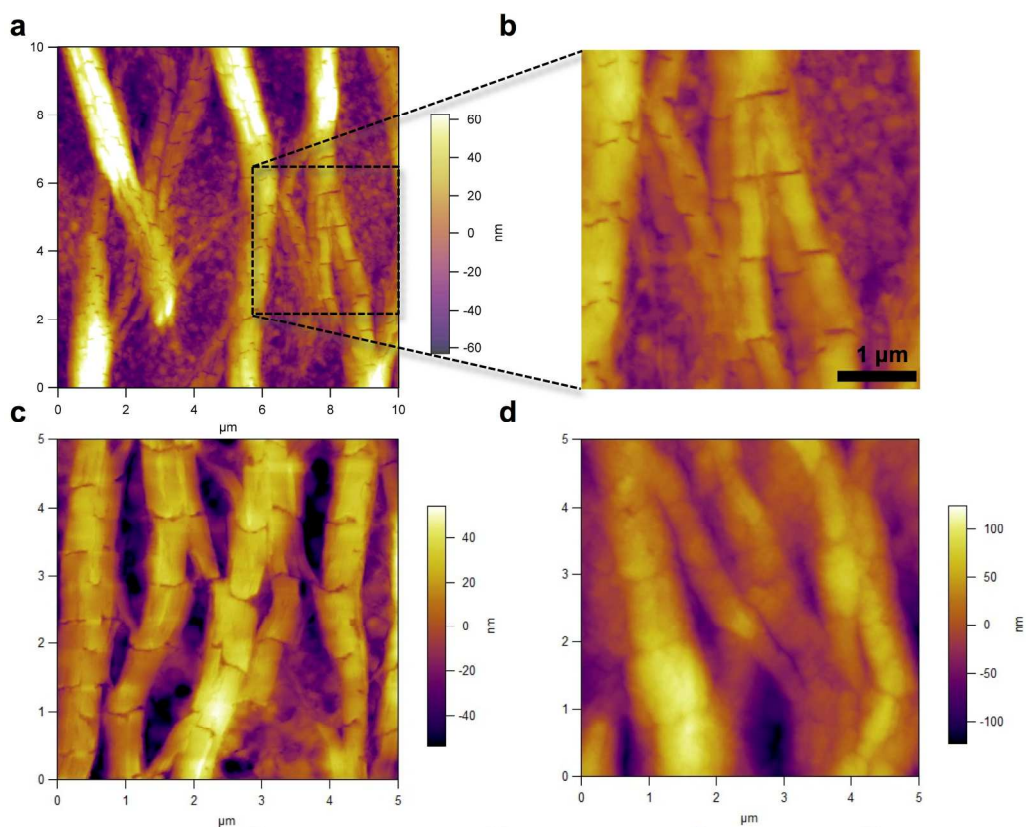


Figure S1. AFM analysis of columnar smectic phage-bundled nanostructures. (a) AFM analysis showed that the phage bundles were composed of multiple columnar smectic nanofibers. **(b)** An enlarged AFM image showing the formation of hierarchical phage nanostructures. **(c)** An AFM image of the phage bundle nanostructure fabricated with Tween20-assisted self-templating process shows relatively loosely spaced nanofilaments. **(d)** This is in contrast to the nanostructure present in phage bundles fabricated in the absence of Tween20.

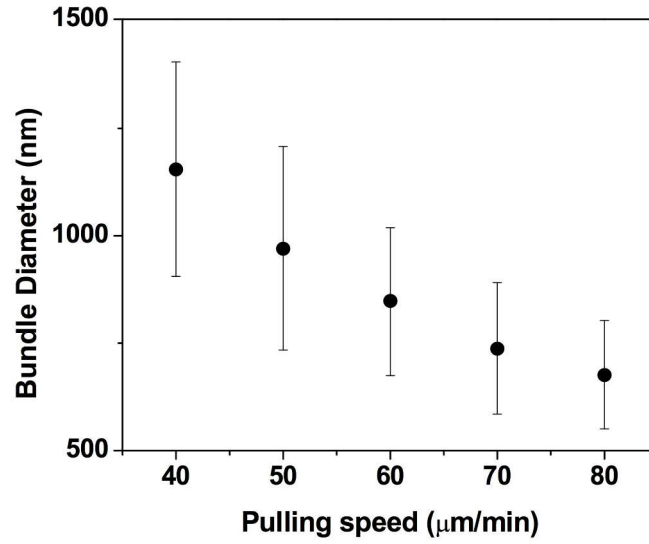


Figure S2. Effect of the bundle diameter of phage bundles depending on the pulling speed. Phage bundle diameter decreases with increased pulling speed during self-templating process.

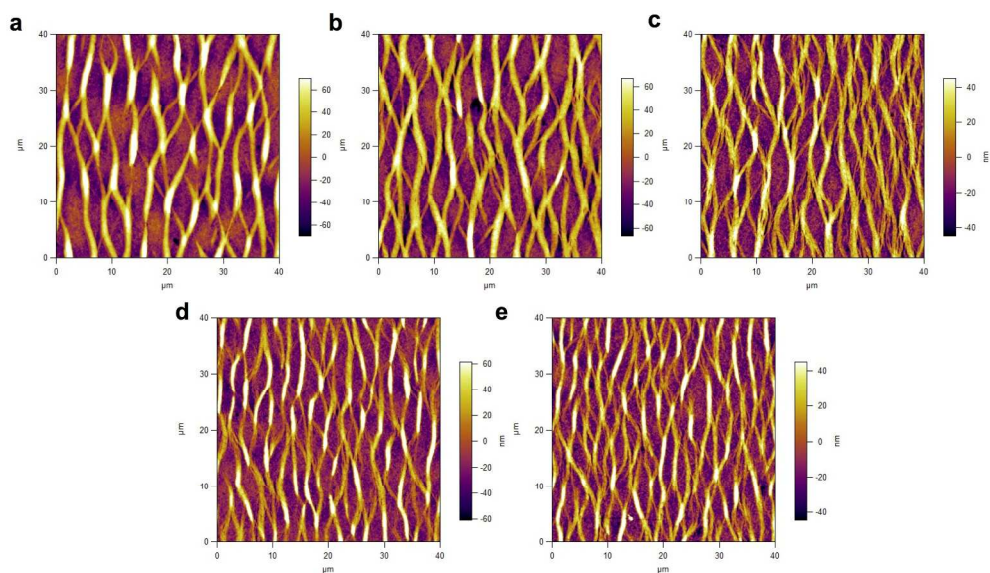


Figure S3. AFM images of phage-bundled nanostructures fabricated with different pulling speeds during self-templating process. Pulling speed of each image: (a) 40, (b) 50, (c) 60, (d) 70, and (e) 80 $\mu\text{m}/\text{min}$, respectively.

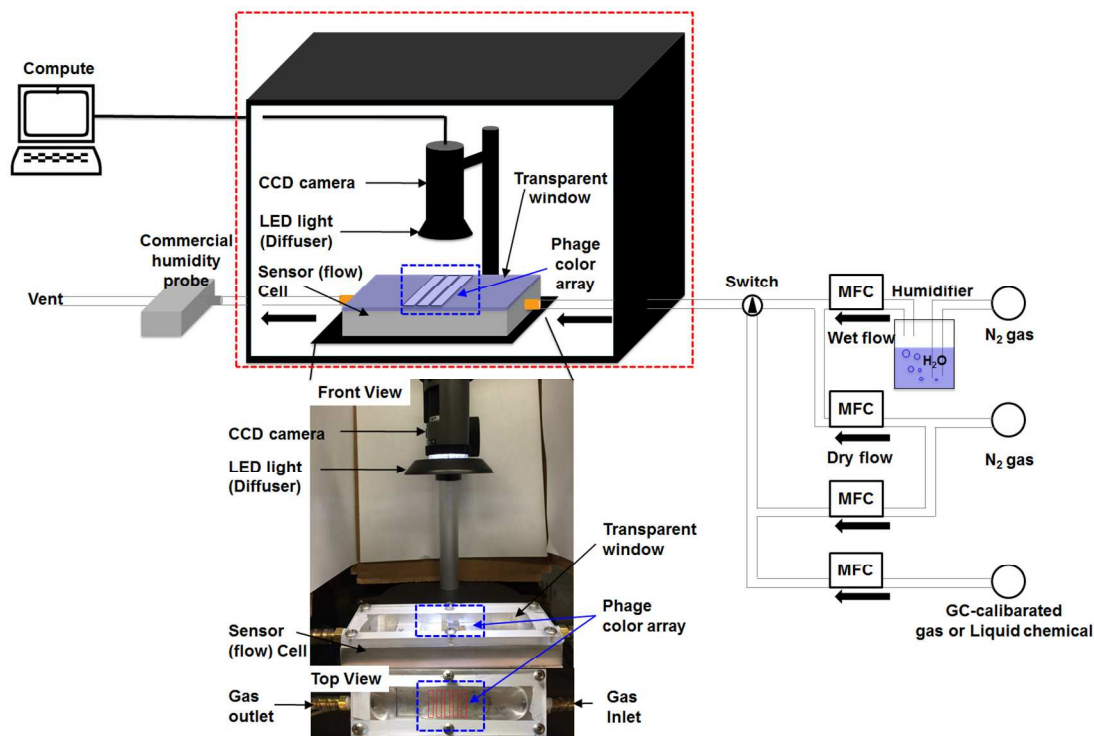


Figure S4. Gas sensing experiment setup using phage-based color matrix array coupled with CCD camera. Phage color sensor array was implemented with a CCD camera based sensor analysis system. The phage sensing matrices were housed within an aluminum sensor cell. The top of the sensor cell was covered with transparent window for unobstructed imaging. The target gases were prepared in a controlled manner by using digital multi-flow controllers (MFC) connected with desired gases. The resulting gases were applied to the phage color array matrices (blue dotted box). The image of phage color array was taken by computer controlled CCD camera with fixed light source. Photographs showed front view and top view of imaging and sensor cell setup. As shown in the red box, the setup was in the dark, close system to prevent interference from stray light. The gas inlet of sensor cell was connected to the gas mixing rig, and the outlet was connected to a commercial humidity sensor to monitor relative humidity before venting the gases.

Parameters	Value	Parameters	Value
Brightness	100	Saturation	20
Contrast	14	Sharpness	1
Hue	0	Gamma	64
Luma	100	Image capture rate	1 image per second

Table S1. Camera imaging parameters.

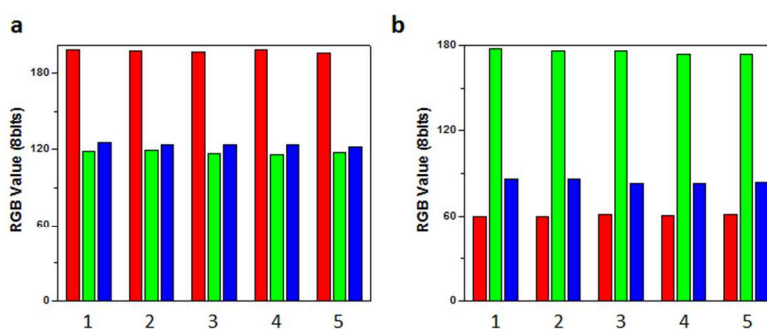


Figure S5. Homogeneity of calibrated colors on representative phage color films. 5 measurements of R, G, B values of representative phage color films after calibration; (a) 3E phage film with 20 μm/min pulling speed, (b) 4E phage film with 20 μm/min pulling speed under constant environmental conditions. A program code, written in MATLAB, was used to control the camera settings to the parameters set in Table S1. Additionally, a reference gray card allowed for white balancing to significantly reduce the uncertainty depending on lighting conditions. Therefore, the resulting digitized and calibrated RGB values of phage color film were consistent.

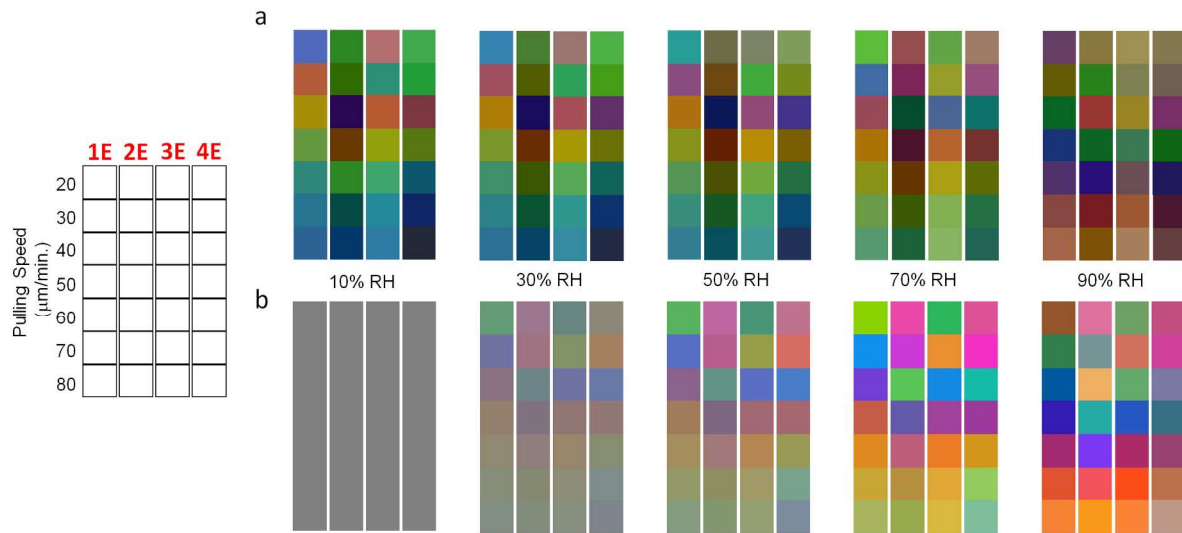


Figure S6. Colorimetric patterns on phage sensor array for various levels of relative humidity (RH). (a) Fingerprint color patterns of phage color matrices for various levels of RH. (b) Difference patterns of phage color sensor array can be generated for each RH level. Each array in difference pattern exhibited color difference to 10% RH (i.e., the average R, G, and B value difference between each RH level and 10%RH. Each layer (R, G, B) = $(R_{128} + (R_{\text{each}} - R_{10\% \text{ RH}}), G_{128} + (G_{\text{each}} - G_{10\% \text{ RH}}), B_{128} + (B_{\text{each}} - B_{10\% \text{ RH}}))$. R_{128} , G_{128} , and B_{128} are backgrounds).

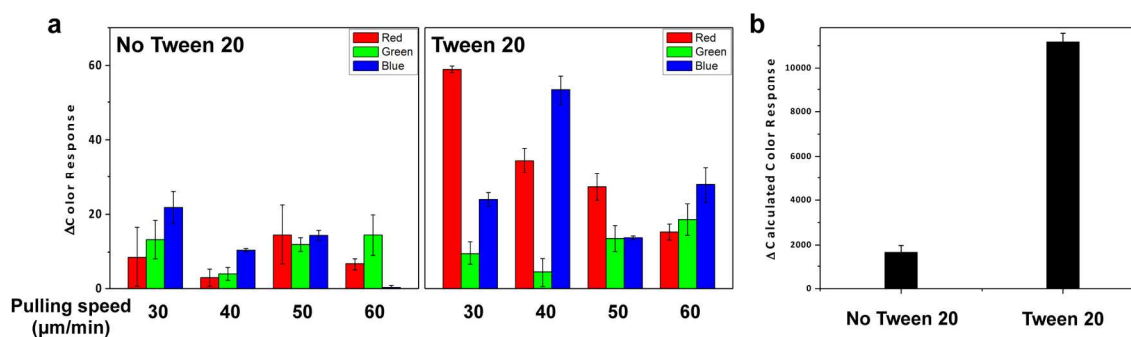


Figure S7. Effect of Tween20 on the sensitivity of the phage color sensor. Presence of Tween20 during self-templating process enhances phage sensor colorimetric responses. **(a)** Genetically engineered quaternary glutamate (4E) phage sensors were created with 4 distinct pulling speeds in the presence and absence of Tween20 during self-templating. The Δ Color Response, the difference in measured RGB values between 10% and 40% RH, was significantly higher across all conditions in sensors developed with Tween20-assisted self-templating process. **(b)** Δ calculated color response from phage color pattern represented squared Euclidean distance. The phage color array with Tween20 exhibited 6.7 times more response than that without Tween20.

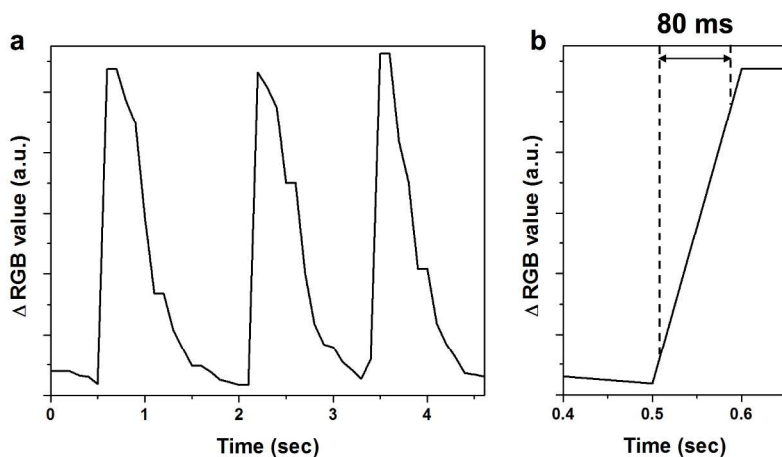


Figure S8. Real time colorimetric responses of the phage color sensors. (a) The phage sensor exhibits fast color change responses as the local %RH is toggled between 5% and 80% over a few seconds. **(b)** The sensors exhibit a <100 ms response time even with an extremely large change in %RH from 10% to 90% of Δ RGB value.

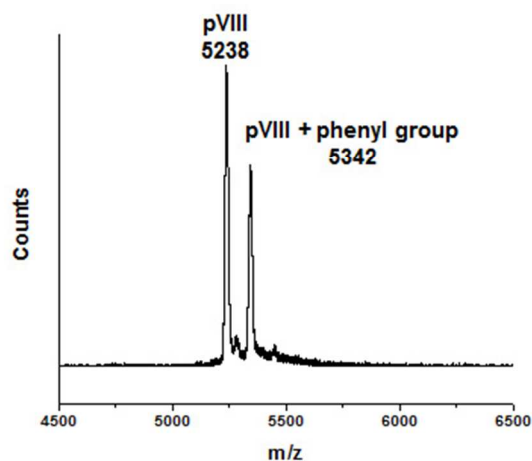


Figure S9. MALDI-TOF MS of unmodified pVIII protein, and chemically modified phenyl-pVIII. The chemical conversion ratio of phenyl-modified pVIII to total pVIII was measured by MALDI-TOF MS and calculated based on the peak intensity of pVIII and pVIII + phenyl group.

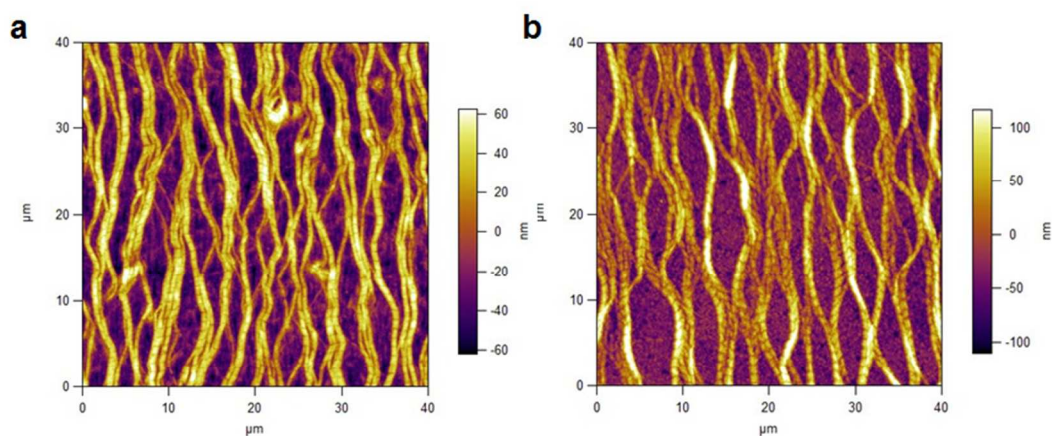


Figure S10. Columnar smectic nanostructures of aromatic group functionalized phage film. Genetically and chemically engineered phage film exhibit columnar smectic nanostructures that are the same as the nanostructure of glutamate engineered phage. (a) AFM image of columnar smectic bundles of chemically modified phage with phenyl groups. (b) AFM image of columnar smectic bundles of genetically engineered WHW phage.

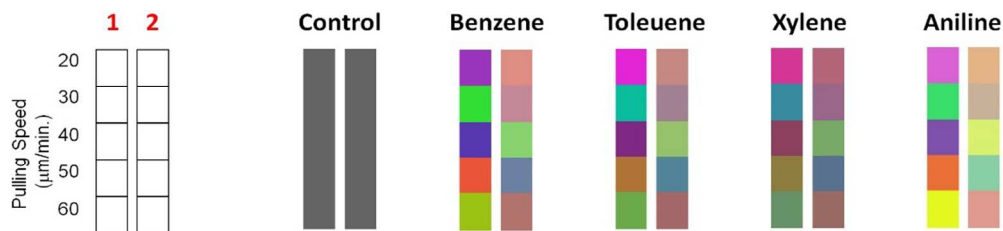


Figure S11. Difference patterns on Colorimetric phage sensor array for benzene, toluene, xylene, and aniline. Difference patterns of phage color sensor array can be generated for each chemical. Each array in difference pattern exhibited color difference from control (*i.e.*, the average R, G, and B value difference between each chemical and control. Each layer (R, G, B) $= (R_{100} + (R_{\text{each}} - R_{\text{control}}), G_{100} + (G_{\text{each}} - G_{\text{control}}), B_{100} + (B_{\text{each}} - B_{\text{control}}))$. R_{100} , G_{100} , and B_{100} are backgrounds.

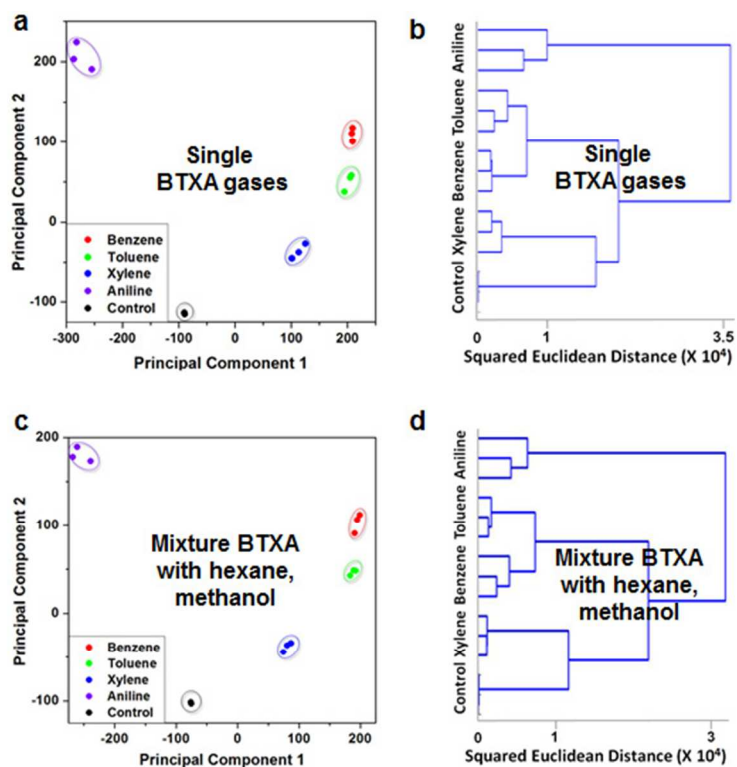


Figure S12. Selective response of phage color sensor arrays to benzene, toluene, xylene, and aniline (BTXA) in single gas and mixture gases conditions. (a) Principal component analysis of the results from three separate experiments using each pure target analyte (*i.e.*, BTXA) and ambient air control (adapted from Figure 4b). (b) Hierarchical Clustering Analysis (HCA) of the phage color sensors upon exposure to pure target analyte (*i.e.* BTXA) and ambient air control (adapted from Figure 4c). (c) Principal component analysis of the results from three separate experiments using each target analyte (*i.e.*, BTXA) in hexane and methanol vapor background. The phage color sensor also responded and generated identical color pattern selectively to target analyte (*i.e.*, BTXA) in mixture conditions. (d) Hierarchical Clustering Analysis (HCA) of the phage color sensors upon exposure to target analyte (*i.e.*, BTXA) mixed with hexane and methanol vapors.

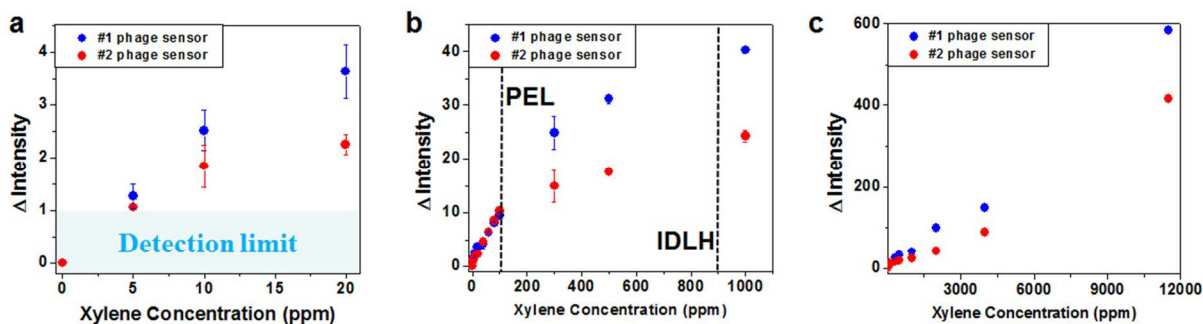


Figure S13. Detection limit and calibration curves of phage color sensor arrays for xylene. (a) #1 phage sensor: wild-type phage with chemically-engineered benzoic acid residues on their major coat protein (pVIII), #2 phage sensor: genetically engineered phage containing WHW-peptides on their major coat protein. The Δ intensity, the sum of difference in absolute values of measured RGB values in 10 phage color arrays between control and given concentration of xylene. The resulting phage color patterns could distinguish 5 ppm of xylene, which is 20-time dilution of permissible exposure limit (PEL) level of xylene. The detection limit was assumed to be three standard deviations from baseline noise in the absence of analytes. (b) Calibration curves from 0 to 1000 ppm, which covers PEL level (100 ppm) and immediately dangerous to life and health (IDLH) level (900 ppm). (c) Calibration curves from 0 to saturated vapor level at room temperature.

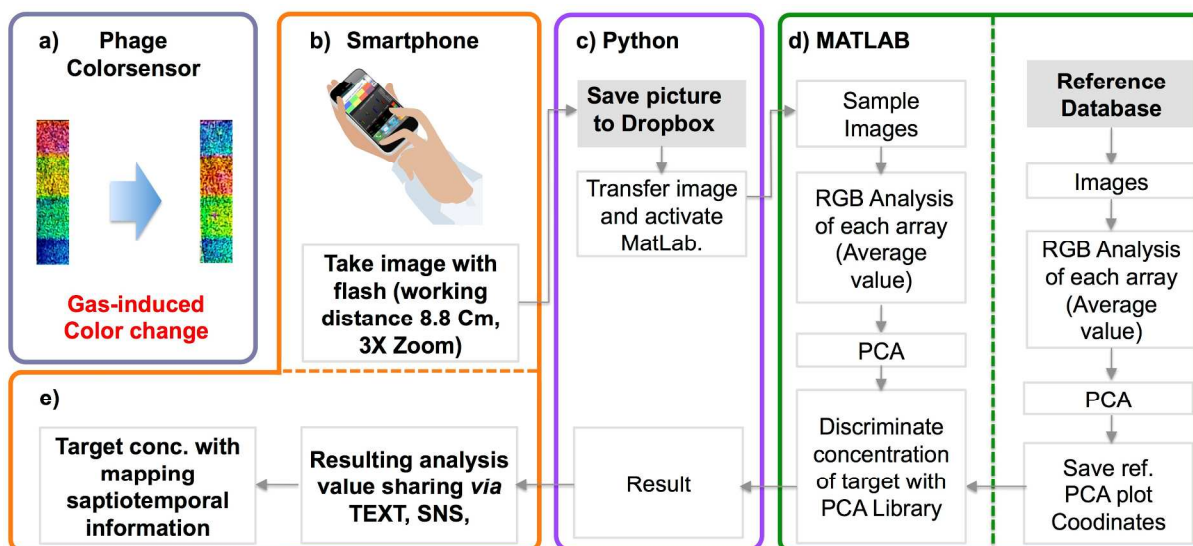


Figure S14. Workflow of smartphone-based phage color sensor analysis and information sharing. (a) A cross-reactive phage color sensor comes into contact with a target analyte and exhibits a unique color change that is species- and concentration-dependent. (b) An image of the sensor is captured by an iOS or Android smartphone and automatically uploaded to a folder on Dropbox using the Dropbox app. (c) A script written in Python detects the newly uploaded image, and initiates MATLAB analysis on that image. (d) MATLAB quantifies the RGB components across a series of distinct phage matrices in the target image and converts these to principal component analysis (PCA) coordinates with a coefficient matrix. These coordinates are compared against those in a database containing coordinates from previously uploaded images captured under known conditions (references). The most similar references are identified, and the concentration of the species that yielded the colors in the new image is estimated by linear interpolation. These results are output by MATLAB. (c, e) A script written in Python couples these MATLAB results with spatiotemporal data obtained from the metadata in the image file and disseminates the sensor information back to the smartphone user or to other relevant people/populations through SMS text messaging, email, or social media such as Twitter.